ELSEVIER

Modern plastic solar cells: materials, mechanisms and modeling

Ryan C. Chiechi[1,2,*], Remco W.A. Havenith[2], Jan C. Hummelen[1,2], L. Jan Anton Koster[2] and Maria A. Loi[2]

[1] Stratingh Institute for Chemistry, University of Groningen, Nijenborgh 4, 9747AG Groningen, The Netherlands
[2] Zernike Institute for Advanced Materials, University of Groningen, Nijenborgh 4, 9747AG Groningen, The Netherlands

We provide a short review of modern 'plastic' solar cells, a broad topic that spans materials science, physics, and chemistry. The aim of this review is to provide a primer for non-experts or researchers in related fields who are curious about this rapidly growing field of interdisciplinary research. We introduce the basic concepts of plastic solar cells and design rules for maximizing their efficiency, including modern quantum chemical calculations that can aide in the design of new materials. We discuss the history of the materials and modern trends in polymeric donor materials and fullerene acceptors, and provide demonstrative data from hybrid polymer/quantum dot devices.

Introduction

This short review provides an overview of research on organic photovoltaic (OPV) devices and many of the materials used in their construction. The sharp rise in societal interest in carbon-neutral, green energy technology in the 21st century has spurred a commensurate rise in research into OPV materials. The volume of this research, which spans chemistry, physics, and materials science, is too great to review in detail in one paper, thus our intent is to give an overview that can serve as an entry point for non-experts into the field or as a guide for researchers in tangential fields who have a general interest in OPV materials research. We focus on two broad categories of OPV devices, 'plastic' solar cells comprising a conjugated polymer and a fullerene acceptor and hybrid organic–inorganic solar cells that blend inorganic semiconductors into organic materials, and the basic principles of designing and understanding new materials and devices. For brevity, we omit small-molecule OPV devices, which are functionally nearly equivalent to polymer-based devices, and direct the reader to recent publications on this topic [1–3].

Photovoltaic cells use the energy of absorbed photons to generate free charge carriers (holes and electrons) which can do electrical work. Organic photovoltaic cells are photovoltaic devices that accomplish this conversion of energy using organic materials – either entirely or as part of a blend [4]. In all cases, at least one of the charge carriers traverses a bulk organic material. Silicon-based (and many other inorganic-based) photovoltaic devices generate free carriers directly from the absorption of a photon, but presently known organic materials do not screen charges as effectively as silicon (because of their lower dielectric constant), which introduces extra steps in the mechanism. In modern OPV devices, the absorption of a photon creates an exciton (i.e. a bound electron-hole pair) which must then be split into free carriers before it decays back to the ground-state, thus OPV devices are 'excitonic' solar cells. This scission process takes place at the interface between the two constituent materials, a donor and an acceptor. These materials are chosen such that energy offsets between the energy levels exist, thus making charge transfer energetically favored (Figure 1a). These materials can be layered or intimately mixed, provided there is a continuous pathway for both holes and electrons to traverse toward the electrodes. Figure 2 is a cartoon of a typical architecture for an OPV device with an inset showing the four basic steps of the exciton scission process at the interface between the donor and acceptor (in reality, many different phases exist in the heterojunction, the cartoon is simplified for clarity). (I) A photon is absorbed by either the donor or the acceptor, creating an exciton. (II) The exciton then diffuses to the interface between the donor and the acceptor. (The distance over which an exciton can travel before decaying is the exciton

*Corresponding author: Chiechi, R.C. (r.c.chiechi@rug.nl)

1369-7021/06/$ - see front matter http://dx.doi.org/10.1016/j.mattod.2013.07.003

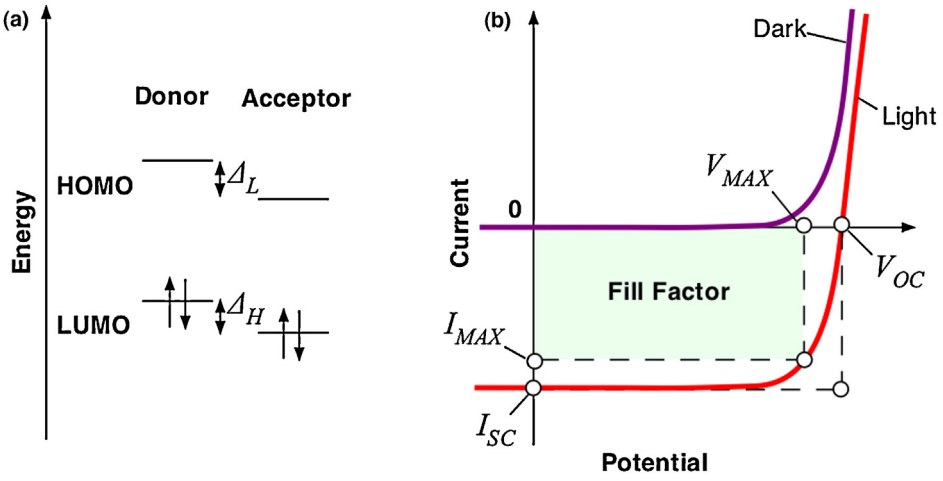

FIGURE 1

(a) Band diagram of a donor–acceptor combination showing HOMO and LUMO offsets. (b) Typical current–voltage characteristics of organic solar cells in dark and under illumination.

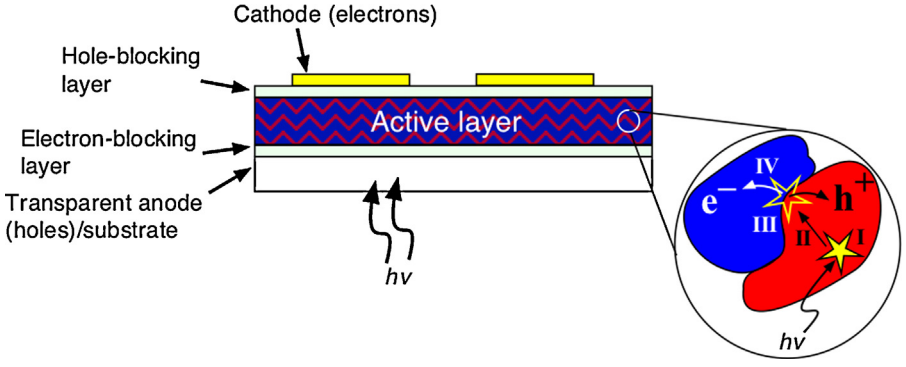

FIGURE 2

A cartoon of an organic photovoltaic device. The active layer comprises the donor and acceptor materials. The inset is a schematic of the scission of an exciton at the interface between the donor (red) and acceptor (blue) materials. (I) The absorption of a photon creates and exciton. (II) The exciton delocalizes to the donor/acceptor interface. (III) A charge-transfer state is created between the two materials. (IV) The charge transfer state dissociates into free carriers which then diffuse into the bulk.

diffusion length.) (III) When the exciton reaches the interface, an electron is transferred to the acceptor (or a hole is transferred onto the donor) creating a so-called charge-transfer (CT) state in which the charges reside on different molecules, but remain bound to each other by coulombic attraction. (IV) The charges overcome this attraction and the CT state dissociates into two free charge-carriers, an electron (e^-) and a hole (h^+), which then travel into the bulk, and eventually into the electrodes. The drift-direction of the charge-carriers is influenced by a difference in work function of the two metallic contacts, which can be further optimized by introducing blocking layers [5]. Hole and electron blocking layers are not present in all OPV devices, but are becoming increasingly common in architectures in which both the donor and the acceptor are in contact with both electrodes. The cathode material has historically been a low work function metal such as Ca or Al and the anode/substrate of a thin film of poly(ethylenedioxythiophene):poly(styrenesulfonate) (PEDOT:PSS) on tin-doped indium oxide (ITO) on glass or a transparent polymer substrate, but neither is particularly well suited for deployment in commercial devices, which require solution-processable electrode materials (e.g. silver inks).

Design rules

It is the excitonic nature of OPV devices that introduces challenges that are not present in silicon-based devices. For example, the nature of the CT state is not fully understood [6], nor is the exact mechanism of dissociation into free carriers. Furthermore, the broadband nature of the solar spectrum can lead to a complex set of charge separation mechanisms that may operate simultaneously, depending on the materials combinations and the morphology of the heterojunction. These challenges are rooted in the complex nature of organic materials for which slight variations in their packing and orientation in the solid-state give rise to substantially different properties. One can design a material with favorable optical properties – a large oscillator strength, broadband absorption, among others. – but current organic materials (usually) form excitons that have a limited lifetime and therefore a limited diffusion length. The relatively low dielectric constants of organic materials that gives rise to the excitonic mechanism also favors charge recombination, either geminate, when formed by absorption of the same photon (i.e. the initial CT state) while they are still weakly bound to each other across the interface or bimolecular (non-geminate), when free carriers annihilate each other.

There are no straightforward design rules for mitigating these losses – at least in terms of the specific chemical structure of the materials – but there are general rules for maximizing the external power conversion efficiency (PCE η) of an OPV device [7].

An OPV device is measured by sweeping a voltage range in the dark and under AM 1.5 G illumination (AM is the standard air mass, $1/cos\,\theta$, $\theta = 48^\circ$ relative to the azimuth, and G is global, which accounts for diffuse, off-axis light). A cartoon of these *I/V* curves is shown in Figure 1b. The key parameters derived from these curves are the open-circuit voltage, V_{OC}, the short-circuit current, I_{SC}, and the fill factor, *FF*, from which η can be determined using Eq. (1) where P_{MAX} is the maximum incident power and *A* is the area of the device [8] (Note: Current density, J_{SC}, is often substituted for I_{SC}/A.) The degree to which a device deviates from ideality is captured in *FF*, which is largely a reflection of recombination processes.

$$\eta = FF\frac{I_{SC}V_{OC}}{AP_{MAX}} \quad (1)$$

The current–voltage characteristics and efficiencies of OPV devices are sometimes modeled using an equivalent circuit that places the source of the photocurrent in parallel with a diode and a resistor and in series with another resistor. However, such an approach obscures much of the physics so other models have been developed. Inspired by the observation that many polymer/fullerene solar cells (see below) are characterized by length scales that are smaller than typical device thicknesses (~100–200 nm), a one-dimensional drift-diffusion approach was developed [9]. In this model, the blend of acceptor and donor materials is treated as an effective medium. Despite the neglect of morphology, this modeling approach provided the first quantitative description of organic solar cells in terms of materials properties and basic physics. Several two-dimensional and three-dimensional models have been put forward to deal with morphological issues, both based on drift-diffusion [10–14], as well as, on kinetic Monte-Carlo techniques [15,16]. Finding a suitable description of the morphology is not trivial, but if it is known quantitative agreement can be obtained [14].

Idealized energy offsets for the donor and acceptor are shown in Figure 1a. A very simple approximation of the maximum possible V_{OC} is the difference in energy between the LUMO of the acceptor and the HOMO of the donor. When a photon is absorbed by either material, the resulting exciton will lose an amount of energy equivalent to Δ_H or Δ_L when it dissociates at the donor/acceptor interface however these values cannot be zero because they are the driving force for the dissociation. Empirically, ~0.3 eV is sufficient to drive the scission of excitons [17]. If the difference is smaller, excitons will tend to decay to the ground state. Any excess energy is dissipated and does not contribute to V_{OC}. The upper limit for I_{SC} can be approximated by the overall efficiency of the four steps shown in Figure 2, the transport of the free carriers, and their extraction by the electrodes. It is a reflection of the combined properties of the device, the materials, and the processing and the relaxation of high-energy photons to the band-edge, which is unavoidable. Therefore, V_{OC} is the one parameter that is (nearly) directly relatable to controllable materials properties, that is, the ionization potential and electron affinity of organic materials are synthetically adjustable and can be measured by a variety of means.

Next-generation organic solar cells

Until recently, it was argued that organic solar cells would always be less efficient than inorganic ones with maximum efficiencies of organics limited to 10–11% [7]. These 'design rules' have guided the research in this field for several years. However valuable, the analysis underlying these rules is limited. In a more extended treatment we have recently shown that OSCs can have efficiencies of more than 20% [18]. A key parameter is the screening of charge carriers by using high-ε materials. Light absorption then leads directly to significant numbers of free carriers, avoiding the need to use a large offset between the donor and acceptor energy levels. This mechanism would place organic solar cells on equal footing with their inorganic counterparts.

Donor and acceptor materials

Donors

Although the observation of photoconductivity [19] and eventually the photovoltaic effect in organic molecules [20] dates back to the early 20th century, modern organic photovoltaic began in earnest in 1986 with the 'Tang Cell,' which was a two-layer device comprising a glass/ITO anode supporting a layer of copper phthalocyanine (the donor), a perylene diimide derivative (the acceptor), and a gold cathode [21]. This device yielded $\eta \sim 1\%$ under AM 2 illumination, despite reasonably high values of $FF \sim 0.65$ because it consisted of only a planar donor/acceptor interface; the bulk of the volume of the device carries charges, but does not contribute to I_{PH}. In 1992 a team of researchers at UC Santa Barbara demonstrated photo-induced electron transfer from poly[2-methoxy-5-(2′-ethylhexyloxy)-*p*-phenylene vinylene] (MEH-PPV) to C_{60} [22]. This work demonstrated the principles of the first 'plastic' solar cell an OPV device containing a conjugated organic polymer. A follow-up to this work in 1995 introduced a soluble fullerene derivative, [6,6]-phenyl-C61-butyric acid methyl ester (PCBM) and defined the concept of a (polymer/fullerene) bulk heterojunction (BHJ) an intimate mixture between two materials (usually a conjugated polymer and a fullerene derivative) that creates a high surface area of contact between donor and acceptor materials through spontaneous, nanoscopic phase-segregation, preferably at the scale of the exciton diffusion lengths [23]. That same year, researchers at the University of Cambridge independently observed the formation of BHJs in intimate mixtures of polymers [24]. Virtually all OPV devices – polymer/fullerene, polymer/polymer, hybrid organic/inorganic, among others. – employ the BHJ strategy to optimize the area of the charge-separation interface in the volume of the active layer.

The early plastic solar cells utilized MEH-PPV, which was designed with asymmetric and racemic 2-ethylhexyl side-chains explicitly to make the polymer more glassy (i.e. homogeneous) in the solid state as well as to improve the solubility. That MEH-PPV and a derivative with longer racemic side-chains, poly[2-methoxy-5-(3′,7′-dimethyloctyloxy)-1,4-phenylenevinylene] (MDMO-PPV), performed so well in OPV devices was largely a coincidence that the spacing of the side chains was exactly the right size to allow fullerenes to intercalate, providing close π–π contact between the materials and improved charge transport. Nearly simultaneously McCullough *et al.* developed a straightforward route to regio-regular poly(3-alkylthiophenes) and specifically regio-regular poly(3-hexylthiophene) (rr-P3HT) [25]. Although the band-gap of rr-P3HT is slightly

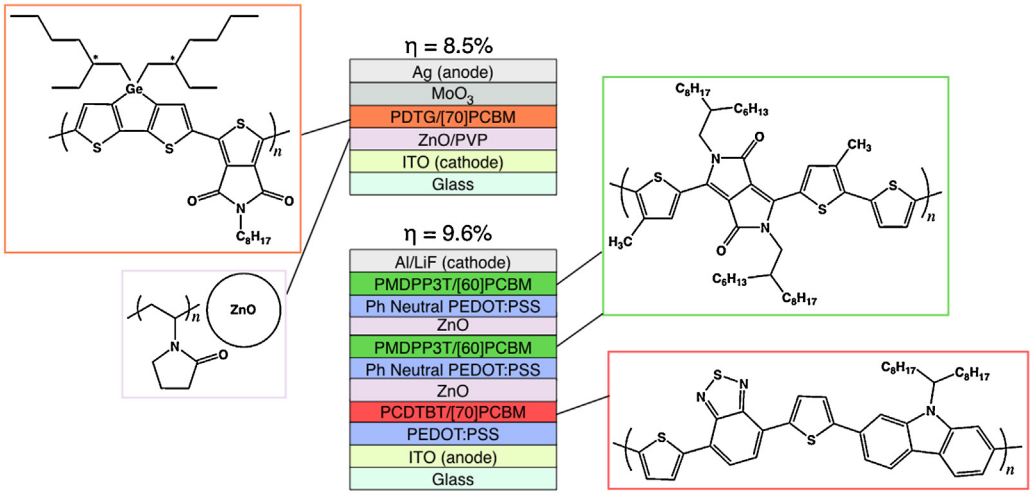

FIGURE 3

A schematic of two exemplary polymer/fullerene OPV devices and the structure of the polymers used in their fabrication from Refs. [29,31]. Top: a single-junction cell in an inverted architecture in which a PVP/ZnO nanoparticle composite serves as an intermediate layer that allows ITO to serve as a cathode. In this configuration, the MoO_3 layer serves the same function as PEDOT:PSS in a non-inverted device. Bottom: a triple-junction device in which three single-layer devices are stacked and wired in series to efficiently harvest a large portion of the visible-to-NIR spectrum.

too large to match the solar spectrum, the Van der Waals interactions of the hexyl side-chains create a strong driving force for the formation of highly crystalline domains and the HOMO and LUMO levels are matched sufficiently (though not perfectly) well to PCBM. The result is an 'ink' of rr-P3HT/PCBM that is capable of producing devices of $\eta \sim 5\%$ with unparalleled reproducibility. Thus it became the benchmark against which materials, fabrication methods, and device architectures are still largely compared [26]. Most modern conjugated polymers pursue the 'weak donor/strong acceptor' strategy combining 'weak donors' with 'strong acceptors' in co-polymers [27]. Here, the terms 'donor' and 'acceptor' are referring to the electron affinities of the co-monomers relative to each other and should not be confused with donors and acceptors in OPV devices; donor/acceptor co-polymers are still hole-carrying, donor materials. The weak (electron) donor pushes the HOMO level up, while the strong acceptor brings the LUMO level down, thus narrowing the band-gap and matching the energy levels of the fullerene acceptor. This strategy has pushed η into the 5–10% range, which recently exceeded 10% in a tandem OPV cell [28].

Figure 3 is a schematic of two exemplary polymer/fullerene OPV devices that capture many of the aspects of modern OPV materials and device design. The top device is inverted, meaning a silver anode collects holes, while the ITO cathode collects electrons [29]. Inverted architectures are desirable for commercialization because they obviate the need for reactive cathode materials, but until recently they have generally lagged behind in efficiency. In this case, efficient inversion is accomplished by using ZnO in poly(vinylpyrrolidone) (PVP) matrix at the cathode and MoO_3 at the anode. This device also incorporates a donor/acceptor co-polymer containing Ge [30]. The use of heteroatoms, particularly the higher chalcogens and carbon group elements, in conjugated polymers is an increasingly common strategy that influences bond lengths and angles and interchain interactions without negatively impacting the electronic properties. The bottom device in Figure 3 shows a triple-junction architecture, where three single-junction OPV cells are stacked and wired in series [31]. Multi-junction OPV devices benefit from being able to capture different portions of the spectrum with different active layers, allowing each material to be tuned for a specific absorbance range and potentially reducing losses from band-edge relaxation however, balancing the annihilation of charges at each interface is non-trivial and requires optimization for each combination of materials. A broad discussion of various polymer solar cell architectures can be found elsewhere [32].

Acceptors

Despite the recognition of the active role of acceptors in light-harvesting going all the way back to the Tang Cell [21], fullerene acceptors in BHJ plastic PV based on polymer/fullerene combinations were primarily viewed to serve simply as efficient electron acceptor and electron conductor in the blend. As a consequence, the mainstream of materials research in plastic PV has invariably been focused on the development of new and better oligomeric or polymeric donor materials donors with optimized optical bandgap for the AM 1.5 spectrum, with the a hole mobility similar to the electron mobility of [60]PCBM for balanced charge transport, with an optimized LUMO-LUMO offset between that of the polymer and that of [60]PCBM (i.e. Δ_L), good processability, and chemical stability. Nevertheless, with the introduction of [70]PCBM, ten years ago, it was already proven that there is only one fundamental difference between donor and acceptor materials in functioning in a donor/acceptor molecular solar cell: the transport of the type of charge carriers. [70]PCBM (available only as a mixture of isomers, in contrast to [60]PCBM, which is a single compound) is a versatile and strongly blue and green light absorbing acceptor with an electron mobility only slightly less than that of [60]PCBM. The absorption spectrum of [70]PCBM makes it a complementary (to the donor polymer) absorber in almost every world record efficiency plastic solar cell of the past ten years. Hence, under AM 1.5 illumination, absorption and exciton diffusion take place in both phases, leading to both hole and electron transfer processes at the D/A interface [33,34].

The key feature of fullerenes and their solution processable derivatives in the PV active layer is their low internal reorganization energy in every relevant process in which they are involved. This low reorganization energy, the high polarizability of the molecule [35], and the relatively high dielectric constant of the solid [36] ($\varepsilon_r = 4$) are closely related properties that stem from the spherical shape and the size of the π-conjugated system. Hence, the spherical shape, albeit a nightmare to the chemists who try to design efficient (supra)molecular architectures for highly efficient PV action between donor and acceptor molecular systems, is a unique and highly beneficial property for OPV application. While [60]PCBM and [70]PCBM have almost identical and quite versatile optical bandgaps for standard PV application, [84]PCBM is a real low bandgap material that can be employed in IR-sensitive PV devices [37].

As is evident by the challenges surrounding polymer acceptors [38,39], designing superior alternatives to fullerenes is far from trivial, as they will have to surpass a whole set of strong features of [70]PCBM. Nevertheless, especially in the search for ultimately green and high dielectric constant active layer ingredients, non-fullerene acceptors are potentially more viable candidates, at least in the long run.

Hybrid organic–inorganic solar cells

Hybrid photovoltaic devices based on blends of semiconducting polymers and colloidal semiconductor nanocrystals (NCs) [40] represent an emerging technology able to combine the advantages of the two classes of materials the high optical absorbance of conjugated polymers and the high conductance, tunable optical band gap and high dielectric constant of nanocrystals ($\varepsilon = 17$ for PbS and $\varepsilon = 23$ for PbSe) [41–43]. Among the many semiconductor nanocrystals under investigation for photovoltaic applications (CdSe [44,45], CdS [46,47], CdTe [48], PbSe [49–51]), lead sulfide (PbS) NCs [52] have emerged as one of the most promising candidates, because of their high electron mobility [53,54], broad absorption and stability [55,56]. In particular, the synthetic control over the PbS diameter allows for the precise tuning of the quantum confined energy gap [57] enabling solar energy conversion in the near-infrared (NIR) [58]. Moreover, the high quality of PbS NCs allows power conversion efficiencies above 4% with a simple Schottky junction solar cells (metal semiconductor junctions) [59,60]. While hybrid OPV devices are relatively new compared to polymer/fullerene blends, they are rapidly gaining ground.

The stringent requirements for the realization of efficient hybrid blends have limited the performance of the PbS/polymer system until now. Only very recently the Prasad group [61] showed that it is possible to meet all these criteria and to achieve high efficiency in hybrid devices based on PbS NCs. By selecting a suitable narrow band-gap polymer, poly(2,6-(*N*-(1-octylnonyl)dithieno[3,2-*b*:20,30-*d*]pyrrole)-*alt*-4,7-(2,1,3-benzothiadiazole)) (PDTPBT) [62], and performing a post deposition ligand exchange, they realized an energetically favorable type II heterojunction with broad spectral response and a PCE of 2%. Optimization of the devices, by selecting the suitable nanoparticle size and by inserting a titania (TiO_2) interlayer before the cathode deposition, allowed reaching 3.78%. Prasad and co-workers showed the importance of the energy levels matching between the polymer and the nanoparticles, and the efficacy of the post-deposition ligand exchange treatment.

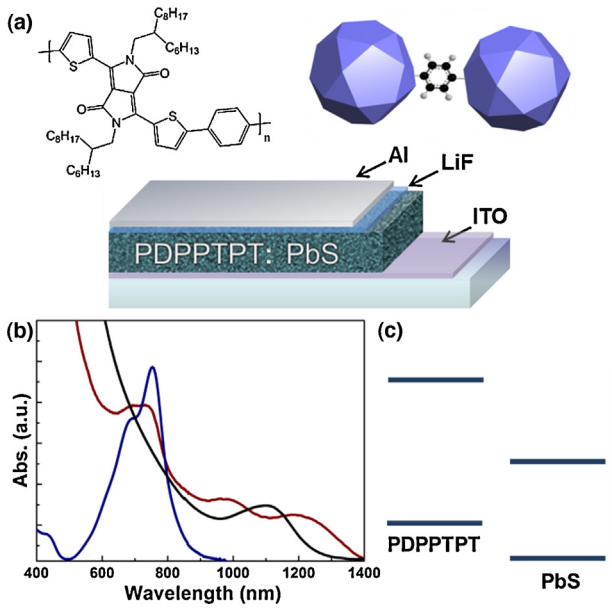

FIGURE 4

Molecular structure of the PDPPTPT polymer, schematic of the BDT crosslinked PbS nanocrystals and of the device structure. [63] Reproduced by permission of the Royal Society of Chemistry

Using a simpler device structure Piliego *et al.* realized efficient bulk heterojunction solar cells with PbS NCs and a narrow band gap polymer, PDPPTPT (poly[{2,5-bis(2-hexyldecyl)-2,3,5,6-tetrahydro-3,6-dioxopyrrolo[3,4-*c*]pyrrole-1,4-diyl}-*alt*-{[2,2′-(1,4-phenylene)bisthiophene]-5,5′-diyl}]) [63].

Using this bulk heterojunction blend produced a simple and efficient hybrid solar cell, as shown in the schematic device configuration in Figure 4. A thin layer of PDPPTPT:PbS-OA (10:90 wt%) blend was deposited on the top of the ITO substrate by spin-coating, followed by the ligand exchange treatment. Optical measurements performed on the blend indicate that the combination of the PbS nanoparticles with this narrow band gap polymer form a type II heterojunction (i.e. Figure 1a) and is expected to provide good photovoltaic performance. Figure 5a shows the *I–V* characteristic of the best PDPPTPT:PbS blend device measured under AM 1.5 illumination at 100 mW/cm^2. The device exhibits a J_{SC} of 12.5 mA/cm^2, V_{OC} of 0.47 V, and a FF of 49% resulting in an overall PCE of 2.9%. This value is remarkable considering the absence of interlayers at the interface with the electrodes. It has been shown that the insertion of a thin hole blocking buffer layer, such as TiO_2 or ZnO [64], on top of the active layer could dramatically improve the performance. Figure 5b compares the incident photon-current conversion efficiency (IPCE) spectrum of the device from the PDPPTPT:PbS blend and the absorption spectrum of the BDT treated blend film. The IPCE spectrum obtained from the device is consistent with the film absorption showing the combined contribution of PDPPTPT and PbS. This proves that blending the narrow band gap polymer and the NIR absorbing PbS NCs gives rise to a broad response covering from the UV to the NIR spectral range.

Progress in device physics

The importance of charge transport in OPV has been widely recognized [65]. If charges cannot be transported out of the active layer sufficiently quickly, there is a real possibility for them to

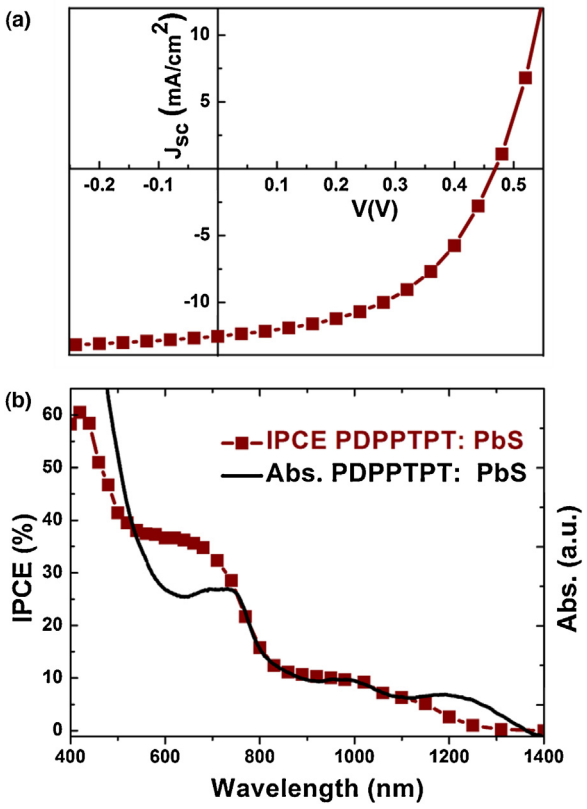

FIGURE 5

(a) *I–V* characteristics of the PDPPTPT:PbS (10/90 wt%) blend under AM 1.5 G (100 mW/cm^2), and (b) plots of the IPCE of the blend device and the absorption spectrum of the BDT-treated blend film. [63] Reproduced by permission of the Royal Society of Chemistry

recombine. Additionally, if one carrier species is much slower than the other one a net space-charge will be built-up in the active layer [65,66]. This space-charge distorts the electric field such that the extraction of the slower species is aided, at the cost of slowing down the extraction of the faster species. The overall process limits the fill-factor and efficiency of solar cells with unbalanced electron and hole mobilities.

Organic materials are characterized by both energetic and positional disorder. Charge transport involves a sequence of hopping events, whereby carriers hop from one localized site to another. Clearly, this is very different from band-type transport in high-quality inorganic semiconductors. It is well known that the mobility of charge carriers in organic materials is a strong function of electric field and carrier density [67]. While there exist several techniques to measure charge transport in one form or another, not all of them are equally suited to OPV materials. To reflect charge transport in OPV devices, the electric field and carrier density need to be representative of real devices. It is therefore not straightforward to use field-effect transistor (FET) data to describe the transport in organic solar cell materials as FETs operate at much higher carrier densities than solar cells do.

Another important realization regards charge transport was the discovery that a donor/acceptor blend can have very different transport properties than their pristine constituents [65]. For example, in PPV/PCBM blends the hole mobility is found to be several orders of magnitude higher than in the pristine PPV material. This behavior is indicative of the ability of interactions between fullerenes and the pendant groups of conjugated polymers to affect π-stacking in the backbone [65].

Charge transport is but one side of the charge-extraction coin. Bimolecular recombination is the other. Whereas bimolecular recombination in organic LEDs follows standard Langevin theory [68], which implies that it is governed by the sum of the mobilities, large deviations have been found in several donor–acceptor blends [69]. Surprisingly, recombination processes are much slower in these blends, which greatly improves the efficiency.

One of the central parameters of organic solar cells is the open-circuit voltage (V_{OC}). Broadly speaking, it is determined by the work functions of the contacts [70], the energy levels of the materials [71] and the carrier generation and recombination processes [71,72]. In 2006, these insights in the device physics of organic solar cells culminated in the prediction that PCEs over 10% could be reached [7,73]. At the time, the highest reported efficiencies were in the 3–4% range and the 10% efficiency mark was far away. However, provided the energy levels of the donors could be tuned to make the combination with fullerenes more favorable, while at the same time improving the overlap with the solar spectrum, it was predicted that organic solar cells could be much more efficient. With the benefit of hindsight, one can safely say that these are indeed key factors in the steady progress in efficiencies that have been reported since.

Electronic structure theory in organic photovoltaic materials

The description of OPV devices is a perfect example where multi-scale modeling is required. It ranges from microscale modeling, with accurate calculations on the individual constituent molecules, to device modeling, where macroscopic properties are used as input, to determine the efficiency of the actual device. The macroscopic properties used here as input can be derived from high-level calculations or from experiment. Complete modeling at the microscopic level of OPV devices is far from straightforward [74] for example, the structures of the devices are usually not known precisely, the size of the system hampers the application of many computational methods, and accurate descriptions of the ground state and the excited states are required, which limits the applicability of computational methods even further. The current strategy is to combine macroscale modeling molecular dynamics with quantum chemical calculations on the molecular scale.

Nowadays, the most studied features are the properties of the electronic ground and excited states of the polymers and oligomers, the morphology and structure of the donor–acceptor interface, the charge-transfer states at the donor–acceptor interface, and the transition rates for different decay pathways. The morphology of the donor–acceptor interface is usually studied using (course grained) molecular dynamics simulations of polymer/PCBM blends. Especially interesting is the morphology as a function of the polymer:PCBM ratio, to find the optimal blending ratio [75]. This optimal blending ratio appears to be quite dependent on the polymers for a P3HT:PCBM blend [75] a phase separation was found for a low PCBM weight percentage, while for a PBTTT:PCBM (PBTTT is a donor/acceptor co-polymer) blend [76] the optimal blending ratio had higher PCBM concentrations because of substantial intercalation of PCBM in PBTTT [77],

leading to a PBTTT-plus-PCBM phase. Also, periodic DFT calculations have been performed to study P3HT/C_{60} interface, and in particular to gain insight in the interfacial charge-transfer mechanism [78]. In this study, it was found that an efficient adiabatic electron transfer is highly probable, because of the presence of an electronic state that extends across the interface in the lowest excited state.

Calculations on molecular systems have been performed to study the rates of electron transfer (see, e.g. [79–83]). The estimation of these rates is based on Marcus and related models [84,85]. Here, the governing matrix element is the electronic coupling between the diabatic initial and final states. One way to calculate this coupling matrix elements is the procedure of Kawatsu *et al.* [86] using the ZINDO/CISD approximation. Another way to evaluate these matrix elements is the use of nonorthogonal CI [87]. The competing singlet–triplet intersystem crossing rate can be estimated using a time-dependent approach [88]. The relative rates of the various possible processes can be used to predict whether charge-separation or recombination is favored at the donor/acceptor interface, guiding the design of new materials for OPV devices.

Combination of molecular dynamics and first principle calculations is nowadays the tool to study the charge-transfer states. Molecular dynamics simulations are performed to generate suitable geometries on which more accurate quantum chemical studies are performed, as has been done in some recent studies [89–91]. This combination of QM/MM was used to rationalize the good electron-hole separation at the P3HT/PCBM interface [90]. It turned out that near the interface, the P3HT chains are more disordered, which led to an increase in the band gap. This enlarged band gap has as a consequence that excitons and holes are repelled by the interface. In another study, the charge-transfer rates as a function of the variations in structure have been studied [89]. One interesting result is that two different interface geometry groups exist, one that supports charge transfer states with complete charge while the other group supports charge bridging states.

Because of size limitations, only DFT and semi-empirical calculations are computationally feasible at the moment. The excitation energies of the donor molecules are frequently calculated using the TDDFT approach, however, current popular functionals are usually not suitable for the calculation of the energies of the charge-transfer states [92,93]. Solutions to overcome this problem are the use of long-range corrected functionals [94,95–97], or constrained DFT calculations [98,99].

The environment can have a significant influence on the energetics of the excitation energies and the energies of the CT and CS states. These effects can be accounted for by using a QM/MM approach: a relatively small part of the system (one PCBM molecule and one oligomer) is treated using a quantum chemical approach, which is embedded in polarizable charges. Different schemes exist, like the Discrete Reaction Field (DRF) approach [100,101], and the polarizable embedding density functional theory scheme [102], which has been used to calculate one- and two-photon absorption in green fluorescent protein [103].

Computational studies on only the polymers are also valuable for investigating the electronic and optical properties of the copolymers [104]. Interestingly, in a study of donor/acceptor polymers, a correlation between the efficiency of OPV devices and the change in dipole moment upon excitation has been found [105]. These dipole moments for ground- and excited states have been calculated at the semi-empirical AM 1 level, using the CIS approach. An alternative way to calculate the dipole moment of excited states is with response theory [106], which may give more reliable results.

Future directions in multi-scale modeling

The advances in computer technology and linear scaling techniques [107,108–110], together with the development of more accurate functionals, make the treatment of large systems at an accurate level computationally realistic. This means that in the near future accurate predictions of the CT states of the molecules are within reach and, that, for the prediction of the electron transfer rates, more accurate electronic couplings together with the Franck-Condon factors can be evaluated using more advanced methods. Embedding techniques with QM/MM methods ensure that influences of the environment are properly taken into account, so that accurate predictions at the micro-scale level can be made. The embedding should be dynamic which means that changes that occur in the environment upon excitation/electron transfer can be taken into account. This will lead to deeper knowledge of the processes that take place at the interface, and will provide detailed information on how the molecular properties of the individual molecules affect the efficiency of the device.

Conclusion

Over the past 25 years, the field of organic photovoltaics has grown from scientific curiosity to viable technology, with both startups and large companies increasingly working to bring 'plastic solar cells' to market. In this short review we touched on bulk heterojunction and hybrid OPV architectures, but there are others, for example, small-molecule, tandem, and bi-layer. However polymer-based, bulk heterojunction OPV devices have already been commercialized and are the most likely to see large-scale production in the near-future, not because they have the highest power conversion efficiencies, but because they can be fabricated reproducibly, roll-to-roll, and without vacuum steps. The principal challenges lie in lowering costs by, for example, finding cheaper printable cathodes and more efficient encapsulation methods to extend the service lifetime of the devices. Current research efforts in interfacial materials and inverted architectures (i.e. that do not require air-sensitive cathode materials) may very well solve some problems, but there is a bright future for all forms of OPV. In the next 25 years, we will probably see myriad OPV architectures in myriad form factors, to fill small, niche applications all the way to large-scale energy production plants.

Acknowledgements

This work is part of the research program of the Foundation for Fundamental Research on Matter (FOM), which is part of the Netherlands Organization for Scientific Research (NWO). This is a publication by the FOM Focus Group 'Next Generation Organic Photovoltaics', participating in the Dutch Institute for Fundamental Energy Research (DIFFER). RWAH acknowledges Prof. Dr. R. Broer (RUG, NL) and Drs. H.D. de Gier (RUG, NL) for fruitful discussions. The authors acknowledge the Zernike Institute for Advanced Materials ('Dieptestrategie' program) for financial support. LJAK acknowledges support by a grant from STW/NWO (VENI 11166).

References

[1] B. Walker, C. Kim, T.-Q. Nguyen, Chem. Mater. 23 (2011) 470–482.
[2] Y. Sun, G.C. Welch, W.L. Leong, C.J. Takacs, G.C. Bazan, A.J. Heeger, Nat. Mater. 11 (2011) 44–48.
[3] B.E. Lassiter, J.D. Zimmerman, A. Panda, X. Xiao, S.R. Forrest, Appl. Phys. Lett. 101 (2012) 063303 (4 pages).
[4] G. Dennler, M.C. Scharber, C.J. Brabec, Adv. Mater. 21 (2009) 1323–1338.
[5] J.H. Seo, A. Gutacker, Y. Sun, H. Wu, F. Huang, Y. Cao, U. Scherf, A.J. Heeger, G.C. Bazan, J. Am. Chem. Soc. 133 (2011) 8416–8419.
[6] C. Piliego, M.A. Loi, J. Mater. Chem. 22 (2012) 4141.
[7] M.C. Scharber, D. Mühlbacher, M. Koppe, P. Denk, C. Waldauf, A.J. Heeger, C.J. Brabec, Adv. Mater. 18 (2006) 789–794.
[8] B. Kippelen, J.-L. Brédas, Energy Environ. Sci. 2 (2009) 251–261.
[9] L.J.A. Koster, et al. Phys. Rev. B 72 (2005) 085205.
[10] C.M. Martin, et al. J. Appl. Phys. 102 (2007) 104506.
[11] K. Maturová, et al. Nano Lett. 9 (2009) 3032.
[12] M. Gruber, et al. Org. Electron. 12 (2011) 1434.
[13] B. Ray, P. Nair, M. Alam, Solar Energy Mater. Solar Cells 95 (2011) 3287.
[14] L.J.A. Koster, et al. Adv. Eng. Mater. 3 (2013) 615–621. http://dx.doi.org/10.1002/aenm.201200787.
[15] P.K. Watkins, A.B. Walker, G.L.B. Verschoor, Nano Lett. 5 (2005) 1814.
[16] R.A. Marsh, C. Groves, N.C. Greenham, J. Appl. Phys. 101 (2007) 083509.
[17] J.D. Servaites, M.A. Ratner, T.J. Marks, Appl. Phys. Lett. 95 (2009) 163302.
[18] L.J.A. Koster, S.E. Shaheen, J.C. Hummelen, Adv. Eng. Mater. 2 (2012) 1246.
[19] A. Pochettino, Accad. Lincei Rend. 15 (1906) 171.
[20] H. Kallmann, M. Pope, J. Chem. Phys. 30 (1959) 585.
[21] C.W. Tang, Appl. Phys. Lett. 48 (1986) 183–185.
[22] N.S. Sariciftci, L. Smilowitz, A.J. Heeger, F. Wudl, Science 258 (1992) 1474–1476.
[23] G. Yu, J. Gao, J.C. Hummelen, F. Wudl, A.J. Heeger, Science 270 (1995) 1789–1791.
[24] J.J.M. Halls, et al. Nature 376 (1995) 498–500.
[25] R.D. McCullough, R.D. Lowe, M. Jayaraman, D.L. Anderson, J. Org. Chem. 58 (1993) 904–912.
[26] M. Leclerc, J.-F. Morin, Design and Synthesis of Conjugated Polymers, John Wiley & Sons, 2010.
[27] H. Zhou, L. Yang, W. You, Macromolecules 45 (2012) 607–632.
[28] J. You, L. Dou, K. Yoshimura, T. Kato, K. Ohya, T. Moriarty, K. Emery, C.-C. Chen, J. Gao, G. Li, Y. Yang, Nat. Commun. 4 (2013) 1446.
[29] C.E. Small, et al. Nat. Photonics 6 (2011) 115–120.
[30] C.M. Amb, et al. J. Am. Chem. Soc. 133 (2011) 10062–10065.
[31] W. Li, A. Furlan, K.H. Hendriks, M.M. Wienk, R.A.J. Janssen, J. Am. Chem. Soc. 135 (2013) 5529–5532.
[32] G. Li, R. Zhu, Y. Yang, Nat. Photon. 6 (2012) 153–161.
[33] M.M. Wienk, J.M. Kroon, W.J.H. Verhees, J. Knol, J.C. Hummelen, P.A. van Hal, R.A.J. Janssen, Angew. Chem. Int. Ed. Engl. 42 (2003) 3371–3375.
[34] A. Bakulin, J.C. Hummelen, M.S. Pshenichnikov, P.H.M. van Loosdrecht, Adv. Funct. Mater. 20 (2010) 1653–1660.
[35] R. Antoine, P. Dugourd, D. Rayane, E. Benichou, M. Broyer, F. Chandezon, C. Guet, J. Chem. Phys. 110 (1999) 9771.
[36] S.L. Ren, et al. Appl. Phys. Lett. 59 (1991) 2678–2680.
[37] A.P. Zoombelt, M. Fonrodona, M.M. Wienk, A.B. Sieval, J.C. Hummelen, R.A.J. Janssen, Org. Lett. 11 (2009) 903–906.
[38] C.R. McNeill, Energy Environ. Sci. 5 (2012) 5653–5667.
[39] E. Zhou, J. Cong, Q. Wei, K. Tajima, C. Yang, K. Hashimoto, Angew. Chem. Int. Ed. 50 (2011) 2799–2803.
[40] D.V. Talapin, J.-S. Lee, M.V. Kovalenko, E.V. Shevchenko, Chem. Rev. 110 (2010) 389.
[41] R. Debnath, O. Bakr, E.H. Sargent, Energy Environ. Sci. 4 (2011) 4870.
[42] P. Reiss, E. Couderc, J. De Girolamo, A. Pron, Nanoscale 3 (2011) 446.
[43] I. Kang, F.W. Wise, J. Opt. Soc. Am. B 14 (1997) 1632.
[44] N. Yaacobi-Gross, M. Soreni-Harari, M. Zimin, S. Kababya, A. Schmidt, N. Tessler, Nat. Mater. 10 (2011) 974.
[45] J.N. de Freitas, I.R. Grova, L.C. Akcelrud, E. Arici, N.S. Sariciftci, A.F. Nogueira, J. Mater. Chem. 20 (2010) 4845.
[46] L.X. Reynolds, T. Lutz, S. Dowland, A. MacLachlan, S. King, S.A. Haque, Nanoscale 4 (2012) 1561.
[47] H.C. Leventis, S.P. King, A. Sudlow, M.S. Hill, K.C. Molloy, S.A. Haque, Nano Lett. 10 (2010) 1253.
[48] W. Yu, H. Zhang, Z. Fan, J. Zhang, H. Wei, D. Zhou, B. Xu, F. Li, W. Tian, B. Yang, Energy Environ. Sci. 4 (2011) 2831.
[49] C.Y. Kuo, M.S. Su, Y.C. Hsu, H.N. Lin, K.H. Wei, Adv. Funct. Mater. 20 (2010) 3555.
[50] W.L. Ma, S.L. Swisher, T. Ewers, J. Engel, V.E. Ferry, H.A. Atwater, A.P. Alivisatos, ACS Nano 5 (2011) 8140.
[51] K.M. Noone, N.C. Anderson, N.E. Horwitz, A.M. Munro, A.P. Kulkarni, D.S. Ginger, ACS Nano 3 (2009) 1345.
[52] H. Fu, S.-W. Tsang, Nanoscale 4 (2012) 2187.
[53] S.-J. Lee, M.V. Kovalenko, J. Huang, D.S. Chung, D.V. Talapin, Nat. Nanotechnol. 6 (2011) 348.
[54] S.Z. Bisri, C. Piliego, M. Yarema, W. Heiss, M.A. Loi, Adv. Mater. (2013), http://dx.doi.org/10.1002/adma.201205041.
[55] J. Tang, K.W. Kemp, S. Hoogland, K.S. Jeong, H. Liu, L. Levina, M. Furukawa, X. Wang, R. Debnath, D. Cha, K.W. Chou, A. Fischer, A. Amassian, J.B. Asbury, E.H. Sargent, Nat. Mater. 10 (2011) 765.
[56] M. Sykora, A.Y. Koposov, J.A. McGuire, R.K. Schulze, O. Tretiak, J.M. Pietryga, V.I. Klimov, ACS Nano 4 (2010) 2021.
[57] F.W. Wise, Acc. Chem. Res. 33 (2000) 773.
[58] M.A. Hines, G.D. Scholes, Adv. Mater. 15 (2003) 1844.
[59] K. Szendrei, W. Gomulya, M. Yarema, W. Heiss, M.A. Loi, Appl. Phys. Lett. 97 (2010) 203501.
[60] K. Szendrei, M. Speirs, W. Gomulya, D. Jarzab, M. Manca, O.V. Mikhnenko, M. Yarema, B.J. Kooi, W. Heiss, M.A. Loi, Adv. Funct. Mater. 22 (2012) 1598.
[61] J. Seo, M.J. Cho, D. Lee, A.N. Cartwright, P.N. Prasad, Adv. Mater. 23 (2011) 3984.
[62] W. Yue, Y. Zhao, S. Shao, H. Tian, Z. Xie, Y. Geng, F. Wang, J. Mater. Chem. 19 (2009) 2199.
[63] C. Piliego, M. Manca, R. Kroon, M. Yarema, K. Szendrei, M. Andersson, W. Heiss, M.A. Loi, J. Mater. Chem. 22 (2012) 24411.
[64] W. Yu, H. Zhang, Z. Fan, J. Zhang, H. Wei, D. Zhou, B. Xu, F. Li, W. Tian, B. Yang, Energy Environ. Sci. 4 (2011) 2831.
[65] P.W.M. Blom, et al. Adv. Mater. 19 (2007) 1551.
[66] V.D. Mihailetchi, J. Wildeman, P.W.M. Blom, Phys. Rev. Lett. 94 (2005) 126602.
[67] W.F. Pasveer, et al. Phys. Rev. Lett. 94 (2005) 206601.
[68] A. Pivrikas, et al. Phys. Rev. B 71 (2005) 125205.
[69] A. Pivrikas, et al. Prog. Photovolt.: Res. Appl. 15 (2007) 677.
[70] V.D. Mihailetchi, L.J.A. Koster, P.W.M. Blom, Appl. Phys. Lett. 85 (2004) 970.
[71] L.J.A. Koster, et al. Appl. Phys. Lett. 86 (2005) 123509.
[72] A. Maurano, et al. Adv. Mater. 22 (2010) 4987.
[73] L.J.A. Koster, V.D. Mihailetchi, P.W.M. Blom, Appl. Phys. Lett. 88 (2006) 093511.
[74] J.-L. Brédas, J.E. Norton, J. Cornil, V. Coropceanu, Acc. Chem. Res. 42 (2009) 1691–1699.
[75] C.-K. Lee, C.-W. Pao, C.-W. Chu, Energy Environ. Sci. 4 (2011) 4124–4132.
[76] C.-K. Lee, C.-W. Pao, J. Phys. Chem. C 116 (2012) 12455–12461.
[77] A.C. Mayer, M.F. Toney, S.R. Scully, J. Rivnay, C.J. Brabec, M. Scharber, M. Koppe, M. Heeney, I. McCulloch, M.D. McGehee, Adv. Funct. Mater. 19 (2009) 1173–1179.
[78] Y. Kanai, J.C. Grossman, Nano Lett. 7 (2007) 1967–1972.
[79] V. Lemaur, M. Steel, D. Beljonne, J.-L. Brédas, J. Cornil, J. Am. Chem. Soc. 127 (2005) 6077–6086.
[80] T. Liu, A. Troisi, J. Phys. Chem. C 115 (2011) 2406–2415.
[81] B.P. Rand, D. Cheyns, K. Vasseur, N.C. Giebink, S. Mothy, Y. Yi, V. Coropceanu, D. Beljonne, J. Cornil, J.-L. Brédas, J. Genoe, Adv. Funct. Mater. 22 (2012) 2987–2995.
[82] Y. Yi, V. Coropceanu, J.-L. Brédas, J. Mater. Chem. 21 (2011) 1479–1486.
[83] Y. Li, T. Pullerits, M. Zhao, M. Sun, J. Phys. Chem. C 115 (2011) 21865–21873.
[84] P.F. Barbara, T.J. Meyer, M.A. Ratner, J. Phys. Chem. 100 (1996) 13148–13168.
[85] J.-L. Brédas, D. Beljonne, V. Coropceanu, J. Cornil, Chem. Rev. 104 (2004) 4971–5003.
[86] T. Kawatsu, V. Coropceanu, A. Ye, J.-L. Brédas, J. Phys. Chem. C 112 (2008) 3429–3433.
[87] R.W.A. Havenith, H.D. de Gier, R. Broer, Mol. Phys. 110 (2012) 2445–2454.
[88] M. Etinski, J. Tatchen, C.M. Marian, J. Chem. Phys. 134 (2011) 154105.
[89] T. Liu, D.L. Cheung, A. Troisi, Phys. Chem. Chem. Phys. 13 (2011) 21461–21470.
[90] D.P. McMahon, D.L. Cheung, A. Troisi, J. Phys. Chem. Lett. 2 (2011) 2737–2741.
[91] S.R. Yost, L.-P. Wang, T. van Voorhis, J. Phys. Chem. C 115 (2011) 14431–14436.
[92] A. Dreuw, M. Head-Gordon, J. Am. Chem. Soc. 126 (2004) 4007–4016.
[93] L. Goerigk, S. Grimme, J. Chem. Phys. 132 (2010) 184103.
[94] T. Körzdörfer, J.S. Sears, C. Sutton, J.-L. Brédas, J. Chem. Phys. 135 (2011) 204107.
[95] L. Pandey, C. Doiron, J.S. Sears, J.-L. Brédas, Phys. Chem. Chem. Phys. 14 (2012) 14243–14248.
[96] D. Jacquemin, V. Wathelet, E.A. Perpete, C. Adamo, J. Chem. Theory Comput. 5 (2009) 2420–2435.
[97] R. Peverati, D.G. Truhlar, Phys. Chem. Chem. Phys. 14 (2012) 11363–11370.
[98] Q. Wu, T. van Voorhis, Phys. Rev. A 72 (2005) 024502.
[99] A.M.P. Sena, T. Miyazaki, D.R. Bowler, J. Chem. Theory Comput. 7 (2011) 884–889.

[100] A.H. de Vries, P.T. van Duijnen, A.H. Juffer, J.A.C. Rullmann, J.P. Dijkman, H. Merenga, B.T. Thole, J. Comput. Chem. 16 (1995) 37–55.
[101] P.T. van Duijnen, M. Swart, L. Jensen, in: S. Canuto (Ed.), Solvation Effects on Molecules and Biomolecules, Springer, 2008, pp. 39–102.
[102] J.M. Olsen, K. Aidas, J. Kongsted, J. Chem. Theory Comput. 6 (2010) 3721–3734.
[103] A.H. Steindal, J.M.H. Olsen, K. Ruud, L. Frediani, J. Kongsted, Phys. Chem. Chem. Phys. 14 (2012) 5440–5451.
[104] L. Pandey, C. Risko, J.E. Norton, J.-L. Brédas, Macromolecules 45 (2012) 6405–6414.
[105] B. Carsten, J.M. Szarko, H.J. Son, W. Wang, L. Lu, F. He, B.S. Rolczynski, S.J. Lou, L.X. Chen, L. Yu, J. Am. Chem. Soc. 133 (2011) 20468–20475.
[106] Y. Luo, D. Jonsson, P. Norman, K. Ruud, O. Vahtras, B. Minaev, H. Ågren, A. Rizzo, K.V. Mikkelsen, Int. J. Quantum Chem. 70 (1998) 219–239.
[107] C. Yam, Q. Zhang, F. Wang, G. Chen, Chem. Soc. Rev. 41 (2012) 3821–3838.
[108] D.R. Bowler, T. Miyazaki, Rep. Prog. Phys. 75 (2012) 036503.
[109] S. Coriani, S. Høst, B. Jansík, L. Thøgersen, J. Olsen, P. Jørgensen, S. Reine, F. Pawlowski, T. Helgaker, P. Salek, J. Chem. Phys. 126 (2007) 154108.
[110] T. Kjærgaard, P. Jørgensen, J. Olsen, S. Coriani, T. Helgaker, J. Chem. Phys. 129 (2008) 054106.